# Modeling of the State Transition Equations of Power Systems with Non-continuously Operating Elements by the RCF Method

**Deok Young Kim** †

**Abstract** - In conventional small signal stability analysis, the system is assumed to be invariant and the state space equations are used to calculate the eigenvalues of the state matrix. However, when a system contains switching elements such as FACTS equipments, it becomes a non-continuous system. In this case, a mathematically rigorous approach to system small signal stability analysis is performed by means of eigenvalue analysis of the system's periodic transition matrix based on the discrete system analysis method. In this paper, the RCF (Resistive Companion Form) method is used to analyze the small signal stability of a non-continuous system including switching elements. Applying the RCF method to the differential and integral equations of the power system, generator, controllers and FACTS equipments including switching devices should be modeled in the form of state transition equations. From this state transition matrix, eigenvalues that are mapped into unit circles can be computed precisely.

**Keywords**: Eigenvalue Analysis, Non-continuous Operating Elements, RCF Method, State Transition Matrix

## 1. Introduction

In modern power systems, FACTS equipments are widely used for an effective power flow control that enables the maximization of transferred power capability and improvement in the economic loading of existing transmission facilities. This trend is facilitated by the technical improvement of high power electronic devices. Aside from these attractive features of FACTS equipment, they also cause negative effects such as distortion of the oscillation modes and newly generated unstable modes after switching actions. These effects are generated by the switching operation of power electronic devices [1, 2].

In conventional small signal stability analysis, the system is assumed to be invariant and the state space equations are used to calculate the eigenvalues of the state matrix. Compared to the transient stability analysis method, which shows mixed results of oscillation modes in time domain, the eigenvalue analysis method has a merit to identify each oscillation mode according to state variables and present useful information such as eigenvector and sensitivity coefficients.

However, when a system contains switching devices such as FACTS equipment, it becomes a non-continuous system. In this case, a mathematically rigorous approach to system small signal stability analysis is by means of eigenvalue analysis of the system's periodic transition matrix based on the discrete system analysis method. The RCF method can be applied to not only continuous systems but also non-continuous systems. The eigenvalues from the conventional state space method and RCF method are exactly the same in continuous systems. But in non-continuous system analysis, the RCF method has a merit of detailed analysis in fluctuations of oscillation modes and newly generated unstable oscillation modes after switching actions. Therefore, the RCF method is a very powerful one to analyze a non-continuous system including switching devices such as FACTS equipment in small signal stability analysis [3, 4].

In this paper, the Resistive Companion Form (RCF) method is used to analyze the small signal stability of a non-continuous system including switching devices. To apply the RCF method in power system small signal stability problems, state transition equations and state transition matrices of power system equipment such as the generator, exciter, governor and power system stabilizer are presented. From these state transition matrices, eigenvalues, which are mapped into unit circles, can be computed. To demonstrate the relative merits of the proposed method, a comparison of system eigenvalues from the conventional state space method and the RCF method are presented for complex systems with two switching devices.

The Transactions of the Trans. KIEE, Vol.54A, No.2, pp.67-72, FEB. 2005: A paper recommended and approved by the Editorial Board of the KIEE Power Engineering Society for translation for the KIEE International Transaction on Power Engineering

† School of Electronic & Information Engineering, Kunsan National University, Korea. (dykim@kunsan.ac.kr)

Received October 26, 2004 ; Accepted December 8, 2004

## 2. Resistive Companion form (RCF) Method

For small signal stability analysis, any power system equipment is described with a set of algebraic differential integral equations. These equations can be arranged in the following general form:

$$\begin{bmatrix} i(t) \\ 0 \end{bmatrix} = \begin{bmatrix} f_1(v(t), \dot{y}(t), v(t), y(t), u(t)) \\ f_2(v(t), \dot{y}(t), v(t), y(t), u(t)) \end{bmatrix} \quad (1)$$

where,

$i(t)$ : vector of terminal currents,
$v(t)$ : vector of terminal voltages,
$y(t)$ : vector of device internal state variables,
$u(t)$ : vector of independent controls

This form includes two sets of equations, which are named external equations and internal equations respectively. The terminal currents appear only in the external equations and the device state variables consist of two sets: external states (i.e. $v(t)$ ) and internal states (i.e. $y(t)$ ).

An example of the above modeling is a switching device represented with linear elements. Between switching actions, the model is described with a linear differential equation of the form:

$$\begin{bmatrix} i(t) \\ 0 \end{bmatrix} = \begin{bmatrix} A_{11} & A_{12} \\ A_{21} & A_{22} \end{bmatrix} \begin{bmatrix} v(t) \\ y(t) \end{bmatrix} + \begin{bmatrix} B_{11} & B_{12} \\ B_{21} & B_{22} \end{bmatrix} \frac{d}{dt} \begin{bmatrix} v(t) \\ y(t) \end{bmatrix} \quad (2)$$

Equation (2) is integrated using a suitable numerical integration method such as the trapezoidal method. Assuming an integration time step h, the result of the integration is manipulated to be in the following form:

$$\begin{bmatrix} i(t) \\ 0 \end{bmatrix} = \begin{bmatrix} Y_{11} & Y_{12} \\ Y_{21} & Y_{22} \end{bmatrix} \begin{bmatrix} v(t) \\ y(t) \end{bmatrix} - \begin{bmatrix} P_{11} & P_{12} \\ P_{21} & P_{22} \end{bmatrix} \begin{bmatrix} v(t-h) \\ y(t-h) \end{bmatrix} - \begin{bmatrix} C_{11} & C_{12} \\ C_{21} & C_{22} \end{bmatrix} \begin{bmatrix} i(t-h) \\ 0 \end{bmatrix} \quad (3)$$

To consider the connectivity constraints among the devices of the system, Kirchhoff's current law is applied to each node of the system. Application of KCL at each node will result in the elimination of all device terminal currents. The overall network equation has the form:

$$\begin{bmatrix} 0 \\ 0 \end{bmatrix} = \begin{bmatrix} Y_{s11} & Y_{s12} \\ Y_{s21} & Y_{s22} \end{bmatrix} \begin{bmatrix} v(t) \\ y(t) \end{bmatrix} - \begin{bmatrix} P_{s11} & P_{s12} \\ P_{s21} & P_{s22} \end{bmatrix} \begin{bmatrix} v(t-h) \\ y(t-h) \end{bmatrix} - \begin{bmatrix} Q_1(t-h) \\ Q_2(t-h) \end{bmatrix} \quad (4)$$

or the equivalent:

$$\begin{bmatrix} v(t) \\ y(t) \end{bmatrix} = \begin{bmatrix} Y_{s11} & Y_{s12} \\ Y_{s21} & Y_{s22} \end{bmatrix}^{-1} \begin{bmatrix} P_{s11} & P_{s12} \\ P_{s21} & P_{s22} \end{bmatrix} \begin{bmatrix} v(t-h) \\ y(t-h) \end{bmatrix} + \begin{bmatrix} Y_{s11} & Y_{s12} \\ Y_{s21} & Y_{s22} \end{bmatrix}^{-1} \begin{bmatrix} Q_1(t-h) \\ Q_2(t-h) \end{bmatrix} \quad (5)$$

Note that the above equation represents the state transition equation for the entire system from time t-h to time t. The above linear equation form is the resistive companion form that results from the trapezoidal integration method. The transition matrix is:

$$\Phi(t, t-h) = \begin{bmatrix} Y_{s11} & Y_{s12} \\ Y_{s21} & Y_{s22} \end{bmatrix}^{-1} \begin{bmatrix} P_{s11} & P_{s12} \\ P_{s21} & P_{s22} \end{bmatrix} \quad (6)$$

Eigenvalue analysis of the transition matrix provides the small signal stability of the system.

In general, we are interested in the transition matrix over at least one period of operation of the system. The proposed method provides an algorithm for the recursive computation of the transition matrix over a desired time period and around the operating conditions of the system. The entire transition matrix over a desired time period can be done by sequential substitution of the transition matrix state variables in each time step. The overall transition matrix has the form:

$$\Phi_T(t_n, t_0) = \Phi_n(t_n, t_{n-1}) \cdot \Phi_{n-1}(t_{n-1}, t_{n-2}) \cdots \Phi_2(t_2, t_1) \cdot \Phi_1(t_1, t_0) \quad (7)$$

where, $\Phi_i(t_i, t_{i-1})$ means the transition matrix of the specified time step.

The location of an eigenvalue of the transition matrix indicates the nature of the mode. In order to interpret the eigenvalues in terms of modal damping factors and natural frequencies, we can use the eigenvalue mapping between the transition matrix eigenvalue and state space eigenvalue. It is known that:

$$\lambda_d = e^{\lambda_c T} = e^{-\alpha T} e^{-\beta T} \quad (8)$$

where, $\lambda_d$ and $\lambda_c$ are the eigenvalues of the transition matrix (i.e. discrete system) and state space matrix (i.e. continuous system) respectively, T is the 60Hz period, and $\lambda_c = -\alpha + j\beta$.

Therefore the eigenvalues of the transition matrix have the effect of mapping those of the state space matrix to the unit circle. It implies that highly damped modes are identified with eigenvalues near the center of the unit circle, stable oscillatory modes are identified with eigenvalues within the unit circle and unstable modes are identified with eigenvalues outside the unit circle.

## 3. Application Examples

To compare the eigenvalues of the transition matrix and the state space matrix, complex systems with two switching devices are investigated. The parameters of the application system are:

$$R_1 = 20[\Omega], R_2 = 40[\Omega], R_3 = 30[\Omega], L_1 = 0.05[H],$$
$$L_2 = 0.1[H], C_1 = 0.2[F], V_s = 110[V], h = 0.0001\,\text{sec}$$

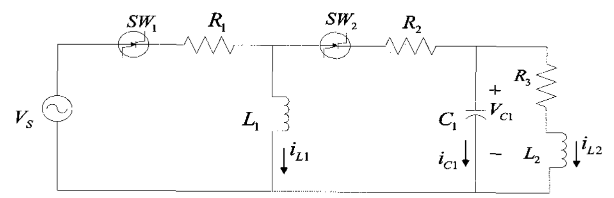


**Fig. 1** Complex system with switching elements

### 3.1 RCF modeling of complex systems

**Case 1 (SW 1: close, SW 2: open)**

From the circuit diagram, the state transition equations are:

$$\begin{bmatrix} 1+\frac{hR_1}{2L_1} & 0 & 0 \\ 0 & 1+\frac{hR_3}{2L_2} & \frac{-h}{2L_2} \\ 0 & \frac{h}{2C_1} & 1 \end{bmatrix} \begin{bmatrix} i_{L1}(t) \\ i_{L2}(t) \\ V_{C1}(t) \end{bmatrix} + \begin{bmatrix} \frac{-hV_s(t)}{2L_1} \\ 0 \\ 0 \end{bmatrix}$$
$$= \begin{bmatrix} 1-\frac{hR_1}{2L_1} & 0 & 0 \\ 0 & 1-\frac{hR_3}{2L_2} & \frac{h}{2L_2} \\ 0 & \frac{-h}{2C_1} & 1 \end{bmatrix} \begin{bmatrix} i_{L1}(t-h) \\ i_{L2}(t-h) \\ V_{C1}(t-h) \end{bmatrix} + \begin{bmatrix} \frac{h}{2L_1}V_s(t-h) \\ 0 \\ 0 \end{bmatrix}$$

**Case 2 (SW 1: open, SW 2: close)**

From the circuit diagram, the state transition equations are:

$$\begin{bmatrix} 1+\frac{hR_2}{2L_1} & 0 & \frac{-h}{2L_1} \\ 0 & 1+\frac{hR_3}{2L_2} & \frac{-h}{2L_2} \\ \frac{h}{2C_1} & \frac{h}{2C_1} & 1 \end{bmatrix} \begin{bmatrix} i_{L1}(t) \\ i_{L2}(t) \\ V_{C1}(t) \end{bmatrix} = \begin{bmatrix} 1-\frac{hR_2}{2L_1} & 0 & \frac{h}{2L_1} \\ 0 & 1-\frac{hR_3}{2L_2} & \frac{h}{2L_2} \\ \frac{-h}{2C_1} & \frac{-h}{2C_1} & 1 \end{bmatrix} \begin{bmatrix} i_{L1}(t-h) \\ i_{L2}(t-h) \\ V_{C1}(t-h) \end{bmatrix}$$

From the above equations, the transition matrix can be calculated as (6).

### 3.2 Comparison of eigenvalues from state space method and RCF method

The eigenvalues of state space method and transition matrix are compared from Table 1 to Table 4. In this example, time step h is also defined as .0001 sec and all the eigenvalues of the state space method are transformed into unit circles in Table 2 and Table 3 while all the eigenvalues of the RCF method are transformed into s-planes in Table 1 and Table 4.

**Table 1** Eigenvalues of Case 1 and Case 2 by state space matrix method (s-plane)

| Mode | Case 1 | Case 2 |
|---|---|---|
| 1 | -0.16675 | -0.29187 |
| 2 | -299.83323 | -299.83312 |
| 3 | -400.0 | -799.87498 |

In Table 1, all the eigenvalues of the state space method in Case 1 and Case 2 are shown in s-plane. It is clear that there are no relations between the eigenvalues of Case 1 and Case 2. This means that it is impossible to analyze the effects of switching actions between Case 1 and Case 2 by the state space method.

**Table 2** Comparison of eigenvalues by state space matrix method and RCF method

| Mode | Eigenvalues of T=0.0006sec ($0 < T < 0.0006$ sec) | | | |
|---|---|---|---|---|
| | State Space Method | | RCF Method | Error Ratio (%) |
| | S-plane | Unit Circle | | |
| 1 | -0.16675 | 0.99989 | 0.99989 | 0.0 |
| 2 | -299.8332 | 0.83535 | 0.83534 | 0.00134 |
| 3 | -399.9999 | 0.78662 | 0.78660 | 0.00318 |

In Table 2, the eigenvalues are calculated at t=0.0006 sec in Case 1 (SW1 is closed and SW2 is opened), which is from 0 to 0.0006 sec with a time step of 0.0001 sec. It is assumed that the errors of the transition matrix by sequential substitution of state variables in each time step

**Table 3** Comparison of eigenvalues by state space matrix method and RCF method

| Mode | Eigenvalues of T=0.001 sec ($0 < T < 0.001$ sec) | | | |
|---|---|---|---|---|
| | State Space Method | | RCF Method | Error Ratio (%) |
| | S-plane | Unit Circle | | |
| 1 | -0.29187 | 0.99988 | 0.99988 | 0.00089 |
| 2 | -299.83312 | 0.88697 | 0.88697 | 0.0 |
| 3 | -799.87498 | 0.72618 | 0.72606 | 0.01706 |

will be the largest at 0.0006 sec. In this case the largest error ratio between state space method and RCF method is 0.00318%, which means that the eigenvalues from the two methods are almost the same.

In Table 3, the eigenvalues are calculated at t=0.001 sec in Case 2 (SW1 is opened and SW2 is closed), which is from 0.0006 to 0.001 sec with a time step of 0.0001 sec. It is also assumed that the errors of transition matrix by sequential substitution of state variables in each time step will be the largest at 0.001 sec. In this case the largest error ratio between state space method and RCF method is 0.01706%, which means that the eigenvalues from the two methods are almost the same.

**Table 4** Eigenvalues of RCF method including switching effect (s-plane)

| Mode | T=.0006 | T =.0007 | T =.0008 | T =.0009 | T =.001 |
|---|---|---|---|---|---|
| 1 | -.16675 | -.1711607 | -.1792794 | -.1876583 | -.1954392 |
| 2 | -299.8332 | -299.8555 | -299.8555 | -299.8555 | -299.8555 |
| 3 | -399.9999 | -457.2448 | -500.1340 | -533.4900 | -560.1738 |

The fluctuations of eigenvalues after switching action by RCF analysis method in each time step are shown in Table 4. All the eigenvalues are transformed into s-planes. To compare the eigenvalues of Tables 1 and 4, the loci of eigenvalues in Table 4 by the RCR method in Case 2 start from those of 0.0006 sec and become closer to those of 0.001 sec in Table 1. It is clear that the fluctuation of eigenvalues in each time step in Table 4 is caused by switching action. These results are impossible to be analyzed by the state space method. To compare the eigenvalues of state space method and RCF method at 0.001 sec, mode 2 is almost identical. But modes 1 and 3 of the state space method and RCF method are very different and the errors of analyzed results are critical.

## 4. RCF modeling of power system equipments

For small signal stability of power systems with non-continuous switching devices by the RCF method, the generator, exciter, PSS and governor are modeled into state transition equations and the state transition matrix of these devices are presented.

### 4.1 Generator full model

The generator full model is used for detailed analysis of generator characteristics or controller actions in one machine infinite bus system.

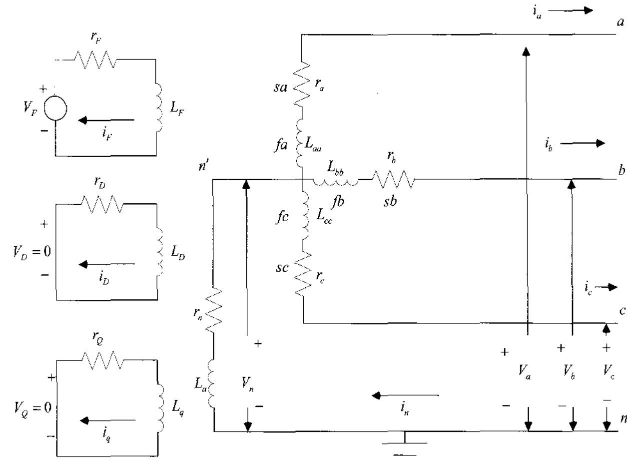


**Fig. 2** Equivalent circuit of full modeled generator

The state transition equations of the generator full model are:

$$\begin{bmatrix} L_d+\frac{h}{2}r & kM_F & kM_D & \frac{h}{2}\omega_0 kL_q & \frac{h}{2}\omega_0 kM_Q & \frac{h}{2}\lambda_{q0} & 0 \\ kM_F & L_F+\frac{h}{2}r_F & M_R & 0 & 0 & 0 & 0 \\ kM_D & M_R & L_D+\frac{h}{2}r_D & 0 & 0 & 0 & 0 \\ \frac{-h}{2}\omega_0 L_d & \frac{-h}{2}\omega_0 kM_F & \frac{-h}{2}\omega_0 kM_D & L_q+\frac{h}{2}r & kM_Q & \frac{-h}{2}\lambda_{d0} & 0 \\ 0 & 0 & 0 & kM_Q & L_Q+\frac{h}{2}r_Q & 0 & 0 \\ \frac{h(\lambda_{q0}-L_d i_{q0})}{6} & \frac{-hkM_F i_{q0}}{6} & \frac{-hkM_D i_{q0}}{6} & \frac{h(-\lambda_{d0}+L_q i_{d0})}{6} & \frac{hkM_Q i_{d0}}{6} & -\tau_j-\frac{h}{2}D & 0 \\ 0 & 0 & 0 & 0 & 0 & \frac{-h}{2} & 0 \end{bmatrix} \begin{bmatrix} i_d(t) \\ i_F(t) \\ i_D(t) \\ i_q(t) \\ i_Q(t) \\ \omega(t) \\ \delta(t) \end{bmatrix} + \begin{bmatrix} \frac{h}{2}v_d(t) \\ \frac{-h}{2}v_F(t) \\ 0 \\ \frac{h}{2}v_q(t) \\ 0 \\ \frac{h}{2}T_m(t) \\ 0 \end{bmatrix}$$

$$= \begin{bmatrix} L_d-\frac{h}{2}r & kM_F & kM_D & \frac{-h}{2}\omega_0 kL_q & \frac{-h}{2}\omega_0 kM_Q & \frac{-h}{2}\lambda_{q0} & 0 \\ kM_F & L_F-\frac{h}{2}r_F & M_R & 0 & 0 & 0 & 0 \\ kM_D & M_R & L_D-\frac{h}{2}r_D & 0 & 0 & 0 & 0 \\ \frac{h}{2}\omega_0 L_d & \frac{h}{2}\omega_0 kM_F & \frac{h}{2}\omega_0 kM_D & L_q-\frac{h}{2}r & kM_Q & \frac{h}{2}\lambda_{d0} & 0 \\ 0 & 0 & 0 & kM_Q & L_Q-\frac{h}{2}r_Q & 0 & 0 \\ \frac{-h(\lambda_{q0}-L_d i_{q0})}{6} & \frac{hkM_F i_{q0}}{6} & \frac{hkM_D i_{q0}}{6} & \frac{-h(-\lambda_{d0}+L_q i_{d0})}{6} & \frac{-hkM_Q i_{d0}}{6} & -\tau_j+\frac{h}{2}D & 0 \\ 0 & 0 & 0 & 0 & 0 & \frac{h}{2} & 0 \end{bmatrix} \begin{bmatrix} i_d(t-h) \\ i_F(t-h) \\ i_D(t-h) \\ i_q(t-h) \\ i_Q(t-h) \\ \omega(t-h) \\ \delta(t-h) \end{bmatrix} + \begin{bmatrix} \frac{-h}{2}v_d(t-h) \\ \frac{h}{2}v_F(t-h) \\ 0 \\ \frac{-h}{2}v_q(t-h) \\ 0 \\ \frac{-h}{2}T_m(t-h) \\ 0 \end{bmatrix}$$

### 4.2 Generator two-axis model

The generator two-axis model is generally used for multi machine system analysis to reduce computing time and load.

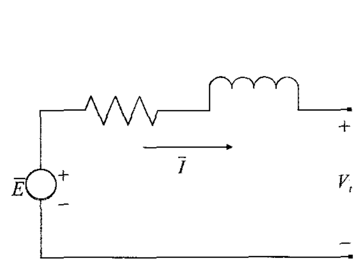


**Fig. 3** Equivalent circuit of two-axis modeled generator

The state transition equations of the generator two-axis model are:

$$\begin{bmatrix} 1+\frac{h}{2\tau'_{d0}} & 0 & 0 & 0 \\ 0 & 1+\frac{h}{2\tau'_{q0}} & 0 & 0 \\ \frac{hI_{q0}}{2\tau_j} & \frac{hI_{d0}}{2\tau_j} & 1+\frac{hD}{2\tau_j} & 0 \\ 0 & 0 & \frac{-h}{2} & 1 \end{bmatrix} \begin{bmatrix} E'_q(t) \\ E'_d(t) \\ \omega(t) \\ \delta(t) \end{bmatrix} + \begin{bmatrix} \frac{-h}{2\tau'_{d0}}[(X_d - X'_d)I_d(t) + E_{FD}(t)] \\ \frac{-h}{2\tau'_{q0}}[(-X_q + X'_d)I_q(t)] \\ \frac{-h}{2\tau_j}[-E'_{q0}I_q(t) - E'_{d0}I_d(t) + T_m(t)] \\ 0 \end{bmatrix}$$

$$= \begin{bmatrix} 1-\frac{h}{2\tau'_{d0}} & 0 & 0 & 0 \\ 0 & 1-\frac{h}{2\tau'_{q0}} & 0 & 0 \\ \frac{-hI_{q0}}{2\tau_j} & \frac{-hI_{d0}}{2\tau_j} & 1-\frac{hD}{2\tau_j} & 0 \\ 0 & 0 & \frac{h}{2} & 1 \end{bmatrix} \begin{bmatrix} E'_q(t-h) \\ E'_d(t-h) \\ \omega(t-h) \\ \delta(t-h) \end{bmatrix} + \begin{bmatrix} \frac{h}{2\tau'_{d0}}[(X_d - X'_d)I_d(t-h) + E_{FD}(t-h)] \\ \frac{h}{2\tau'_{q0}}[(-X_q + X'_d)I_q(t-h)] \\ \frac{h}{2\tau_j}[-E'_{q0}I_q(t-h) - E'_{d0}I_d(t-h) + T_m(t-h)] \\ 0 \end{bmatrix}$$

### 4.3 IEEE type 1 exciter model

IEEE Type 1 is the most generally used exciter model and the block diagram is shown in Fig. 4.

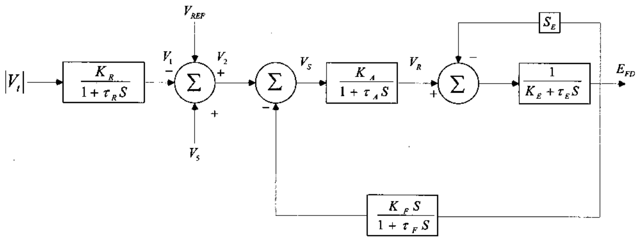


**Fig. 4** Block diagram of IEEE Type 1 Exciter

The state transition equations of IEEE Type 1 exciter are:

$$\begin{bmatrix} 1+\frac{h}{2\tau_E}(S'_E+K_E) & 0 & 0 & \frac{-h}{2\tau_E} \\ 0 & 1+\frac{h}{2\tau_R} & 0 & 0 \\ \frac{h\omega_R K_F(S'_E+K_E)}{2\tau_F\tau_E} & 0 & 1+\frac{h}{2\tau_F} & \frac{-h\omega_R K_F}{2\tau_F\tau_E} \\ 0 & \frac{hK_A}{2\tau_A} & \frac{hK_A}{2\tau_A} & 1+\frac{h}{2\tau_A} \end{bmatrix} \begin{bmatrix} E_{FD}(t) \\ V_1(t) \\ V_3(t) \\ V_R(t) \end{bmatrix} + \begin{bmatrix} 0 \\ \frac{-hK_R}{2\tau_R}|V_t(t)| \\ 0 \\ \frac{-hK_A}{2\tau_A}[V_{REF}(t)+V_S(t)] \end{bmatrix}$$

$$= \begin{bmatrix} 1-\frac{h}{2\tau_E}(S'_E+K_E) & 0 & 0 & \frac{h}{2\tau_E} \\ 0 & 1-\frac{h}{2\tau_R} & 0 & 0 \\ \frac{-h\omega_R K_F(S'_E+K_E)}{2\tau_F\tau_E} & 0 & 1-\frac{h}{2\tau_F} & \frac{h\omega_R K_F}{2\tau_F\tau_E} \\ 0 & \frac{-hK_A}{2\tau_A} & \frac{-hK_A}{2\tau_A} & 1-\frac{h}{2\tau_A} \end{bmatrix} \begin{bmatrix} E_{FD}(t-h) \\ V_1(t-h) \\ V_3(t-h) \\ V_R(t-h) \end{bmatrix} + \begin{bmatrix} 0 \\ \frac{hK_R}{2\tau_R}|V_t(t-h)| \\ 0 \\ \frac{hK_A}{2\tau_A}[V_{REF}(t-h)+V_S(t-h)] \end{bmatrix}$$

### 4.4 Governor model

The block diagram of governor model used is in Fig. 5.

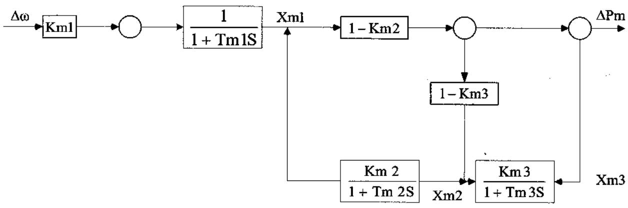


**Fig. 5** Block diagram of governor

The state transition equations of the governor model are:

$$\begin{bmatrix} 1+\frac{h}{2\tau_{m1}} & 0 & 0 \\ \frac{-hK_{m2}}{2\tau_{m2}} & 1+\frac{h}{2\tau_{m2}} & 0 \\ 0 & \frac{-hK_{m3}}{2\tau_{m3}} & 1+\frac{h}{2\tau_{m3}} \end{bmatrix} \begin{bmatrix} X_{m1}(t) \\ X_{m2}(t) \\ X_{m3}(t) \end{bmatrix} + \begin{bmatrix} \frac{hK_{m1}}{2\tau_{m1}}\omega(t) \\ 0 \\ 0 \end{bmatrix}$$

$$= \begin{bmatrix} 1-\frac{h}{2\tau_{m1}} & 0 & 0 \\ \frac{hK_{m2}}{2\tau_{m2}} & 1-\frac{h}{2\tau_{m2}} & 0 \\ 0 & \frac{hK_{m3}}{2\tau_{m3}} & 1-\frac{h}{2\tau_{m3}} \end{bmatrix} \begin{bmatrix} X_{m1}(t-h) \\ X_{m2}(t-h) \\ X_{m3}(t-h) \end{bmatrix} + \begin{bmatrix} \frac{-hK_{m1}}{2\tau_{m1}}\omega(t-h) \\ 0 \\ 0 \end{bmatrix}$$

### 4.5 Power system stabilizer model

The block diagram of power system stabilizer model used is shown in Fig. 6.

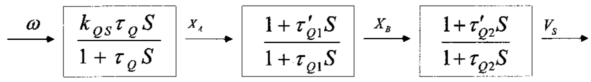


**Fig. 6** Block diagram of power system stabilizer

The state transition equations of PSS are:

$$\begin{bmatrix} 1+\frac{h}{2\tau_Q} & 0 & 0 \\ \frac{-h}{2\tau_{Q1}}(1-\frac{\tau'_{Q1}}{\tau_Q}) & 1+\frac{h}{2\tau_{Q1}} & 0 \\ \frac{-h\tau'_{Q2}}{2\tau_{Q1}\tau_{Q2}}(1-\frac{\tau'_{Q1}}{\tau_Q}) & \frac{-h}{2\tau_{Q2}}(1-\frac{\tau'_{Q2}}{\tau_{Q1}}) & 1+\frac{h}{2\tau_{Q2}} \end{bmatrix} \begin{bmatrix} X_A(t) \\ X_B(t) \\ V_S(t) \end{bmatrix} + \begin{bmatrix} -K_{QS}\omega(t) \\ \frac{-\tau'_{Q1}}{\tau_{Q1}}K_{QS}\omega(t) \\ \frac{-\tau'_{Q1}\tau'_{Q2}}{\tau_{Q1}\tau_{Q2}}K_{QS}\omega(t) \end{bmatrix}$$

$$= \begin{bmatrix} 1-\frac{h}{2\tau_Q} & 0 & 0 \\ \frac{h}{2\tau_{Q1}}(1-\frac{\tau'_{Q1}}{\tau_Q}) & 1-\frac{h}{2\tau_{Q1}} & 0 \\ \frac{h\tau'_{Q2}}{2\tau_{Q1}\tau_{Q2}}(1-\frac{\tau'_{Q1}}{\tau_Q}) & \frac{h}{2\tau_{Q2}}(1-\frac{\tau'_{Q2}}{\tau_{Q1}}) & 1-\frac{h}{2\tau_{Q2}} \end{bmatrix} \begin{bmatrix} X_A(t-h) \\ X_B(t-h) \\ V_S(t-h) \end{bmatrix} + \begin{bmatrix} -K_{QS}\omega(t-h) \\ \frac{-\tau'_{Q1}}{\tau_{Q1}}K_{QS}\omega(t-h) \\ \frac{-\tau'_{Q1}\tau'_{Q2}}{\tau_{Q1}\tau_{Q2}}K_{QS}\omega(t-h) \end{bmatrix}$$

## 4. Conclusion

The state transition equations of power system equipment are presented for applying the RCF method to the systems with non-continuous operating switching devices in small signal stability analysis. The RCF method can be applied to not only continuous systems but also non-continuous systems. The eigenvalues from conventional state space method and RCF method are exactly the same in continuous systems. But in non-continuous system analysis, the RCF method has a merit of detailed analysis in fluctuations of oscillation modes and newly generated unstable oscillation modes after switching actions. Therefore, the RCF method is a very powerful one to analyze non-continuous systems including switching devices such as FACTS equipments in small signal stability analysis of power systems.


## Acknowledgements

This work has been supported by KESRI (R-2003-B-465), which is funded by MOCIE (Ministry of Commerce, Industry and Energy).


## References


[1] "FACTS overview", IEEE power engineering society, 95TP 108, 1995.

[2] Bohmann L. J., Lasseter R. H., "Stability and harmonics in thyristor controlled reactors," IEEE Trans. on Power delivery, Vol. 5, No. 2, pp. 1175-1181, April 1990.

[3] Yousin Tang, A. P. Sakis Meliopoulos, "Power system small signal stability analysis with FACTS elements," IEEE Trans. of power delivery, Vol. 12, No. 3, pp. 1352-1361, July 1997.

[4] Eugene V. Solodovnik, George J. Cokkinides, A. P. Sakis Meliopoulos, "On stability of implicit numerical methods in nonlinear dynamical systems simulation," Proceedings of the 30th southeastern symposium on system theory, pp. 27-31, West Virginia, March 1998.


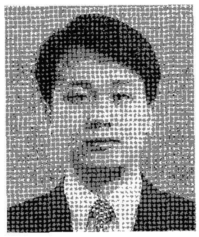


**Deok Young Kim**

He received his B.S., M.S. and Ph.D. degrees in Electrical Engineering from Korea Univ., Korea, in 1988, 1990 and 1996, respectively. He has been an Associate Professor at the School of Electronic & Information Engineering, Kunsan National University since 1996. He was a Post-doctoral Fellow at the Georgia Institute of Technology for one year beginning August 2001. His research interests include FACTS analysis and control, power system modeling and small signal stability analysis.